BRAIN COMMUNICATIONS

High-rate leading spikes in propagating spike sequences predict seizure outcome in surgical patients with temporal lobe epilepsy

Mohamad Shamas, Hsiang J. Yeh, Itzhak Fried, Jerome Engel Jr and Richard J. Staba

Inter-ictal spikes aid in the diagnosis of epilepsy and in planning surgery of medication-resistant epilepsy. However, the localizing information from spikes can be unreliable because spikes can propagate, and the burden of spikes, often assessed as a rate, does not always correlate with the seizure onset zone or seizure outcome. Recent work indicates identifying where spikes regularly emerge and spread could localize the seizure network. Thus, the current study sought to better understand where and how rates of single and coupled spikes, and especially brain regions with high-rate and leading spike of a propagating sequence, informs the extent of the seizure network.

In 37 patients with medication-resistant temporal lobe seizures, who had surgery to treat their seizure disorder, an algorithm detected spikes in the pre-surgical depth inter-ictal EEG. A separate algorithm detected spike propagation sequences and identified the location of leading and downstream spikes in each sequence. We analysed the rate and power of single spikes on each electrode and coupled spikes between pairs of electrodes, and the proportion of sites with high-rate, leading spikes in relation to the seizure onset zone of patients seizure free ($n = 19$) and those with continuing seizures ($n = 18$). We found increased rates of single spikes in mesial temporal seizure onset zone (ANOVA, $P < 0.001$, $\eta^2 = 0.138$), and increased rates of coupled spikes within, but not between, mesial-, lateral- and extra-temporal seizure onset zone of patients with continuing seizures ($P < 0.001$; $\eta^2 = 0.195$, 0.113 and 0.102, respectively). In these same patients, there was a higher proportion of brain regions with high-rate leaders, and each sequence contained a greater number of spikes that propagated with a higher efficiency over a longer distance outside the seizure onset zone than patients seizure free (Wilcoxon, $P = 0.0172$). The proportion of high-rate leaders in and outside the seizure onset zone could predict seizure outcome with area under curve = 0.699, but not rates of single or coupled spikes (0.514 and 0.566). Rates of coupled spikes to a greater extent than single spikes localize the seizure onset zone and provide evidence for inter-ictal functional segregation, which could be an adaptation to avert seizures. Spike rates, however, have little value in predicting seizure outcome. High-rate spike sites leading propagation could represent sources of spikes that are important components of an efficient seizure network beyond the clinical seizure onset zone, and like the seizure onset zone these, too, need to be removed, disconnected or stimulated to increase the likelihood for seizure control.

David Geffen School of Medicine at UCLA, Los Angeles, CA 90095, USA

Correspondence to: Richard J. Staba, PhD
Reed Neurological Research Center
710 Westwood Plaza, Room 2145, Los Angeles, CA 90095, USA
E-mail: rstaba@mednet.ucla.edu

Keywords: temporal lobe; seizure recurrence; spike coupling; spike rate; intracranial electroencephalography

Received April 10, 2023. Revised August 14, 2023. Accepted October 23, 2023. Advance access publication October 24, 2023
Published by Oxford University Press on behalf of the Guarantors of Brain 2023.

Graphical Abstract

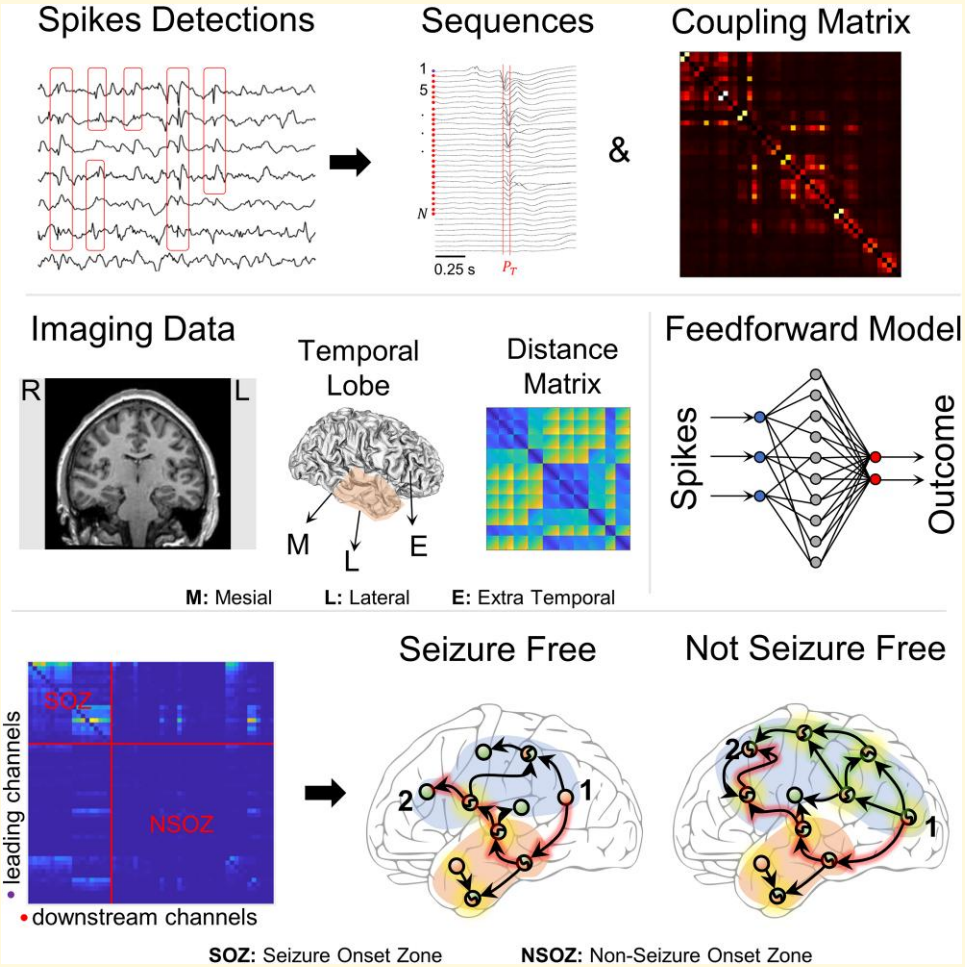

Introduction

The EEG is an important test for the diagnosis and treatment of epilepsy. In patients with medication-resistant seizures who are candidates for surgery, the location of scalp-, and if needed depth EEG-, recorded seizure onsets, indicating the seizure onset zone or SOZ helps to plan the resection. Inter-ictal EEG spikes (herein referred to as spikes), which are distinct phenomena from seizures,[1] also can be used, but the reliance on spikes is lower than seizures because electrodes with frequent spikes can localize in, as well as outside, the SOZ.[2-4] Further, studies show surgical patients with temporal lobe epilepsy who had infrequent unilateral spikes often had better seizure outcomes than those with frequent or bilateral spikes,[5-7] yet others did not.[8,9] The inconsistent results could be due to differences in aetiology, incomplete understanding of the pathophysiology of spikes or the measure of spikes, which often is based on the rate at each electrode contact and might not accurately represent the functional disturbance(s) critical to the seizure network.

Similar to studies of seizures, network analysis is used to study spikes and different approaches have been applied to assess where spikes begin and propagate in relation to the SOZ.[10-13] Results show electrodes with highest rate of spikes are not always in the SOZ, but near to it, and the area where spikes propagate often overlaps with the SOZ.[11,12] In some cases, the locations where spikes emerge from or spread to are the same as those for ictal discharges.[10,14] Overall, results suggest electrodes with frequent spikes that are the source of propagation could be useful to localize the seizure network[4,10,12] and predict seizure outcome.[13]

To further our understanding of spikes in relation to the seizure network, we studied the spatiotemporal characteristics of spikes to answer the following questions. Does the rate of spikes on individual electrodes or the rate of coincident or coupled spikes between pairs of electrodes correspond with the location of the SOZ? Do electrodes with frequent spikes that contain the first or leading spike in a propagated series, which we termed high-rate leaders or hiRL, only reside in the SOZ? Can the rate of spikes or proportion of hiRL or do both equally predict seizure outcome? Answers to these questions derive from a quantitative analysis of spikes and propagation recorded on depth electrodes implanted in patients with medication-

resistant temporal lobe epilepsy who subsequently had surgery to treat their seizure disorder.

Materials and methods

Subjects and clinical recordings

Patients in the current retrospective study were part of a previous study,[15] but the objectives and analysis are different between the previous and current work. Patients had medication-resistant focal seizures who were candidates for epilepsy surgery but required an invasive EEG test to localize the brain area where seizures began. All patients were bilaterally implanted with 7- to 9-contact clinical depth electrodes (Ad-Tech Medical Instrument, Oak Creek, WI) oriented perpendicular to the lateral surface of the temporal bone and positioned in mesial temporal lobe regions such as amygdala, entorhinal cortex, hippocampus and para-hippocampal gyrus, as well as extra-temporal areas including, but not limited to, orbitofrontal cortex, anterior cingulate gyrus and supplementary motor areas. Patients were recorded for 7–14 days in the hospital to capture a sufficient number of habitual seizures, which were reviewed by the attending neurologist to identify the electrode contacts where seizures first appeared. These contacts were labelled as the seizure onset zone (SOZ) and all remaining electrode contacts were labelled non-SOZ (NSOZ). All patients provided informed consent before the implantation of depth electrodes and participating in this research, which was approved by the UCLA Medical Institutional Review Board 3 (10-001452).

Depth electrode recordings and localization

Inter-ictal depth EEG recordings were reviewed to remove signals containing non-EEG noise and the remaining signals notched filtered at 60 Hz to remove powerline interference. Postoperative CT scans were registered to preoperative MRIs to localize the electrode contacts, and those contacts fully in white matter were excluded from the analysis. Analysis was performed on EEG recorded from 1644 noise-free electrode contacts (M: 50 ± 15 contacts per patient) positioned in the gray matter. For each patient a 10- to 60-min depth EEG segment was selected using the following criteria: (i) more than 24 h after electrode implantation; (ii) before tapering of anti-seizure medications; (iii) at least 6 h before the first recorded seizure and (iv) period of quiet wakefulness with eyes open or closed. The sampling rates were 200 Hz ($n = 29$ patients), 1 kHz ($n = 1$) and 2 kHz ($n = 7$).

Spike detection and connectivity matrices

Spikes were detected in each patient's recording using a power spectrum whitening technique in the Delphos software,[16,17] which was validated visually and quantitatively (Fig. 1A) using 10 patients and from each 5 channels, both randomly selected. Results from the automated Delphos detector were compared to those from an independent, manual detection (see Supplementary Table 1).

The strength of spikes coupling between two channels ch_i and ch_j was determined by summing the spikes appearing simultaneously within a 100 ms window on both channels and dividing by the total duration in seconds. The coupling rate r_{ij} found at the row i and column j of the spikes coupling matrices represented the spikes coupling rate between channels i and j. The broadband power of the spikes was calculated for each recording, then used to construct the spikes coupling power matrices. Coupled spikes power between two channels was defined as the mean of the power of all spikes on both channels appearing simultaneously on both channels within a given window (100 ms). Consequently, the spike coupling power M_{ij} at row i and column j of the spikes coupling power matrix is calculated as follows:

$$M_{ij} = \frac{1}{N}\sum_{k=1}^{N}(p_{ki} + p_{kj})$$

where p_{ki} is the broadband power of the spikes at channel i that appears simultaneously with a spike on channel j whose power is denoted as p_{kj}. N is the total number of coupled spikes between channels i and j.

To compute distance connectivity matrices, first the anatomical MRI image was co-registered with the CT image to mask non-brain areas. Then the masked CT images were thresholded, eroded and Gaussian filtered to identify electrodes locations. The processed CT scans were imported into iElectrodes toolbox[18] where electrode contacts where localized, labelled and indexed. The x, y and z coordinates, in millimeter (mm), for each contact in gray matter was extracted according to the MNI system of coordinates whose origin is at the anterior commissure and has an RAS orientation. The Euclidean distance between each pair of electrodes was then calculated and arranged into a symmetric matrix where the distance d_{ij} found on row i and column j represents the distance between channels i and j.

High power–high rates pairs

To identify functionally connected electrodes in spike generation and their proximity to synchronized spike sources, spikes coupling rates and power matrices were used. Contact pairs with the highest 10% coupled spike rates and power were retained by thresholding both matrices. The common contact pairs in both thresholded matrices were isolated to compare between patient groups (seizure free, SF, and not seizure free, NSF) as well as compare between different brain areas (e.g. mesial and lateral temporal lobe and extra-temporal lobe regions).

Electrode contacts grouping

Electrode contacts were categorized by their location relative to the temporal lobe: mesial (M), lateral (L) and

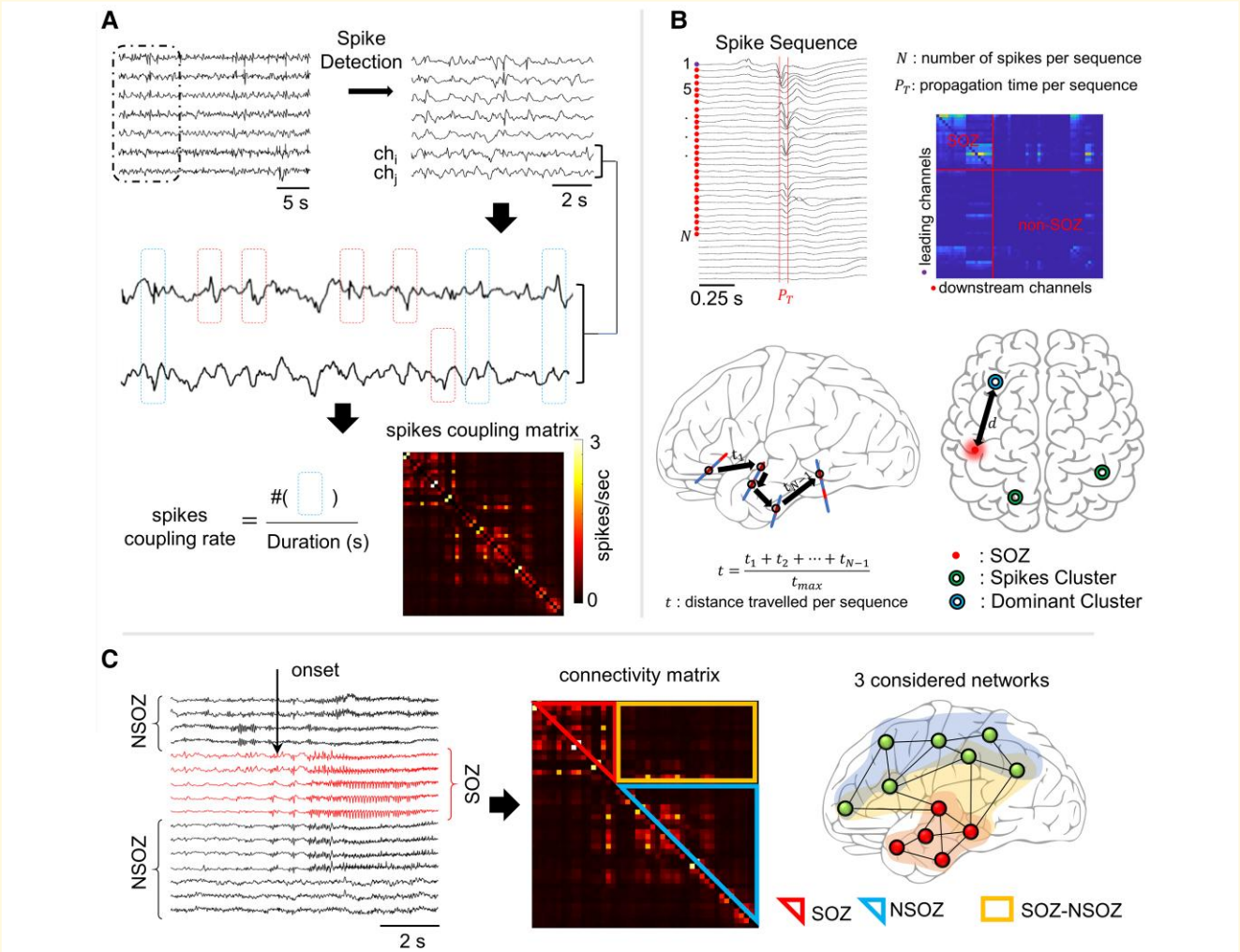

Figure 1 Analysis pipeline. (A) Intracerebral EEG signals are fed to an automatic spike detector (based on spectral whitening) to detect spikes. For each pair of channels ch_i and ch_j coupled spike rate was computed by counting the number of times two spikes appeared synchronously on both channels in a window of 100 ms and dividing by total duration of the signal. Spikes appearing asynchronously on pairs of electrodes were not included. The value r_{ij} at column *i* and row *j* represents the coupled spike rate in spikes/second for channels of indices *i* and *j*. (**B**) Spike sequences are extracted from EEG recordings where the channel whose spike that first appears in time in a particular sequence is considered a leading channel and all the other participating contacts are considered downstream channels. The maximum propagation time allowed (P_{T_max}) was set to 50 ms, all downstream channels should have spikes appearing in a window of 15 ms from the previous sequence-participating channel. Leading-downstream matrices were constructed where each value a_{ij} represents the number of times channel *j* appeared in a spike sequence lead by channel *i*. Trajectory distance *t* travelled by a propagating spike was calculated by adding elementary Euclidean distances between channels with spikes in a particular sequence. Spike sequences were clustered using k-means algorithm, and distance *d* between dominant cluster and seizure onset zone (SOZ) was calculated. (**C**) Classification of connectivity matrices values. Channels first showing seizure onset were classified as seizure onset zone channels, i.e. SOZ. All the other channels were considered non-seizure onset zone channels (NSOZ). The values in each connectivity matrix were classified into three networks, intra-SOZ, intra-NSOZ and inter-SOZ–NSOZ.

extra-temporal (E), i.e. outside the temporal lobe mostly in the frontal lobe and rarely in the parietal and occipital lobe (see Supplementary Table 2 for detailed electrode positioning per patient). Spike functional connectivity networks represented as spikes coupling rates were classified with respect to the SOZ. The SOZ networks included all contacts within the SOZ; NSOZ networks comprised of all contact pairs outside the SOZ, and SOZ–NSOZ network was when one contact was in SOZ and the other in NSOZ (see Fig. 1C).

In regard to brain regions, a similar grouping technique was adopted where all electrode channels labelled either M, L or E produced six possible regional networks, namely: M–M, M–L, M–E, L–L, L–E and E–E. The mean value of spikes coupling rate/power was calculated for each network either in relation to SOZ or in relation with respect to the temporal regions. However, this approach deprived us from the ability to assess the interaction between brain regions and SOZ. For instance, a contact pair that is classified

to be a part of the M–L network has one of its contacts in the mesial and the other in the lateral temporal lobe. At the same time, both contacts can still be a part of the SOZ network. This is not true for all contacts in the M–L networks where some pairs could be a part of the NSOZ or the SOZ–NSOZ network. Hence, calculating the average value for a given brain region network unavoidably disregards the zone networks and vice versa. To evaluate the interaction between anatomical regions and brain zones (SOZ), individual non-averaged coupled spikes measures were considered.

Spikes sequences: temporal and spatial clustering

To identify series of propagated spikes, we used methods adapted from a recently published study.[12] Briefly, the spike that appeared first was labelled as the leader of a propagation sequence and any other spikes on different channels that appeared within 50 ms of the leader or within 15 ms of the last spike were added to the sequence. The window of 50 ms was later expanded to 100 ms producing similar results. As in the previous study,[12] sequences with fewer than 5 spikes or with over 50% of the participating spikes occurring within 2 ms were discarded. Also, distance between electrodes showing spikes of a sequence was taken into consideration to limit propagation velocity to 10 m/s.[19] Contrary to referred study, a visual and quantitative validation of spike detections were performed before spike sequencing. An unsupervised clustering algorithm (k-means) was used to group spikes into clusters by their coordinates. Each cluster was characterized by its position (x, y and z coordinates) and the proportion of spikes per cluster a spike cluster. Clusters were chosen to minimize the Euclidean distance between spikes channels and cluster centroid. The cluster with largest number of spikes was labelled as the 'dominant cluster'. The number of clusters was visually chosen for each patient as the inflection point in a plot of sum of square error as function of cluster number. We used an open-source code with default parameters, available at: https://github.com/erinconrad/spike-propagation.

Propagated spikes and clusters measures

A number of measures were computed to assess aspects of spikes propagation and spikes clusters.

- Average propagation time (P_T) is the difference in time (ms) between the leading and last spikes in a propagated sequence. The average for all sequences was calculated for each patient (see Fig. 1B upper row).
- Total distance travelled per propagated sequence (t): the sum of all Euclidean distances between one channel and preceding channel containing spike in a propagated sequence calculated as t_i, $i = 1 \ldots N-1$, N is number of spikes per sequence, and normalized as the total distance divided by the longest distance between two channels ($t_{\max}$) in each patient (see Fig. 1B lower row).
- Normalized distance between SOZ and dominant cluster (d): computed as the Euclidean distance between centroid x, y and z coordinates of the SOZ and dominant cluster and then normalized by $t_{\max}$ in each patient (see Fig. 1B lower row).
- Normalized distance between SOZ and leading contacts: computed as the average of all distances between the SOZ centroid and leading contact of each spikes propagated sequence and normalized with respect to $t_{\max}$. The average distance is then calculated for each patient.
- Normalized distance between SOZ and high-rate contacts: computed as the average of all distances between the SOZ centroid and each high-rate spikes contact, defined as top 10th percentile of spike rates, and normalized with respect to $t_{\max}$.
- Global efficiency: a single value for each patient computed using the BCT toolbox function[20] that represents the overall inverse of the shortest path length between each pair of contacts in the asymmetrical leading-downstream propagated spikes connectivity matrix, where a sequence containing leader contact i and downstream contact j could have a directed connecting edge from i to j.
- Percentage of high rate to leading contacts (hiRL): in each patient, the electrode contacts that were in the top 10th percentile of spiking rates were identified and the percentage of those contacts that were also leading contacts in at least two spike sequences was calculated. A similar calculation was performed after grouping the contacts according to their location with respect to the SOZ.

Statistical analysis

Multivariate analysis of covariance was used to assess the effects of brain region (M, L and E), SOZ and seizure outcome on spike rate and power, including inter-contact distance as a covariate. All data were tested for normality and non-normal distributions transformed using a Box–Cox function. Data that could not be transformed to a normal distribution were analysed with non-parametric tests. Effect sizes were computed in SPSS as eta squared (η^2) or Cliff's d. Effect size was considered small if $\eta^2 \leq 0.01$, medium $0.01 < \eta^2 \leq 0.14$ and large if $\eta^2 > 0.14$. In all cases, Bonferroni method was used to correct for multiple comparisons when needed. Pearson correlation was used to evaluate the linear relationship between inter-contacts distance and spikes coupling rates/power. All statistical tests were carried out using SPSS software[21] except for the Wilcoxon tests which were performed using the Statistics Toolbox of MATLAB software (The Math Works, Inc., *MATLAB*. Version 2020a). All statistical tests used were two-tailed tests. Analyses were performed objectively using fully automatic detectors and toolboxes, reducing human interference and thus no blinding or randomization was used.

Seizure outcome prediction and validation

A feedforward network model[22] with one hidden layer consisting of 10 neurons was constructed to evaluate measures of spikes to predict seizure outcome. The network was

designed to make predictions based on input features of hiRL or individual spike rates (percentage of hiRL or rate of spikes in SOZ and NSOZ) or coupled spike rates (rates in SOZ, NSOZ, and between SOZ and NSOZ). To validate the performance of the network, a leave-one-out validation method was applied. In case of hiRL, 25 patients were randomly selected and 24 were used to train the model and 1 was used to test the model. To eliminate the possibility of chance results providing a high area under the curve (AUC) value, this process was repeated 1000 times and, in each iteration, 25 patients were randomly drawn from the original 30 patients. A similar approach was used for spike rates, but 30 (29 to train and 1 to test) of the total 37 patients were randomly selected to maintain a comparable percentage of selected to total patients (83%). The performance of the network model was assessed by calculating the area under the receiver operating characteristic (ROC) curve, which provides a measure of the predictive accuracy with values closer to 1 indicating better predictive performance.

Results

Patient cohort

We reviewed 113 patients with medication-resistant focal seizures who required invasive EEG tests to treat their seizure disorder, and we identified 56 with temporal lobe seizures. Of these latter patients, 37 patients ($n = 24$ females; mean age of 37.1 ± 12 years) with focal seizures that began in unilateral ($n = 29$) or bilateral ($n = 6$) mesial temporal lobe or unilateral temporo-parietal ($n = 1$) or -frontal regions ($n = 1$) were included in the current study (Supplementary Table 3). Nineteen were SF with an Engel score of IA or IB and eighteen continued to have seizures (NSF) after resective or RNS surgery (Engel Class IC to IVC) with mean follow-up of 3.12 (±1.9) years. The proportion of females to males and median age at surgery was similar between seizure outcome groups (Mdn: SF 45 versus NSF 39 years old; Wilcoxon test, $P = 0.368$, Cliff's $d = 0.142$). There was no significant difference in frequency of seizures or auras between the SF and NSF groups (Wilcoxon, $P = 0.961$, $d = 0.067$ and $P = 0.787$, $d = 0.256$, respectively). Epilepsy duration, however, was significantly different between the two groups with longer duration of epilepsy in SF than NSF patients (Mdn: 21 versus 9 years; Wilcoxon, $P = 0.017$, $d = 0.358$).

Spatial distribution of spike discharges

The mean spike rate was 4.75 ± 3.9 spikes/min/contact with rates between 0.57 and 18.1 spikes/min/contact. Overall, there was no significant difference in spike rates between NSF and SF patients (non-parametric Wilcoxon test, $P = 0.1468$). In relation to brain region and SOZ, rates were higher in the mesial temporal SOZ of NSF than SF patients ($P < 0.001$; effect size $\eta^2 = 0.138$; Fig. 2A), but no difference in lateral temporal or extra-temporal lobe SOZ ($P = 0.212$ and $P = 0.546$, respectively, Fig. 2A). In addition, mean rates were higher in the mesial temporal NSOZ of NSF than SF patients ($P = 0.033$) but with a very small effect size ($\eta^2 = 0.011$). There was no difference in broadband spike power between NSF and SF patients (Fig. 2C).

Coupled spikes

In contrast to the individual spike rate, coupled spike rates between all pairs of electrode contacts were lower with a mean of 2.56 ± 1.7 spikes/min and rates between 0 and 15.2 spikes/min. Coupled rates were generally higher in NSF than SF patients, and the difference was confirmed statistically after transforming data to a normal distribution (see Supplementary Fig. 1) and adjusting for differences in inter-contact distance (see 'Materials and methods' section). Within mesial (M—M, $P < 0.001$ and $\eta^2 = 0.195$), lateral (L–L, $P < 0.001$ and $\eta^2 = 0.113$), and extra-temporal (E–E, $P = 0.018$ and $\eta^2 = 0.102$) SOZ coupled spike rates were higher in NSF than SF (Fig. 2D). However, coupled rates between different regions (i.e. M–L, M–E and L–E) were similar in NSF and SF patients. Also, in the NSOZ, there was no difference in coupled rates with respect to region or seizure outcome. Coupled spike power showed a significant difference between SF and NSF only when both contacts are in the M–M SOZ where the power of coupled spikes is higher in the SF patients ($P = 0.002$ and $\eta^2 = 0.124$), but in the E–E SOZ, coupled spike power was higher in the NSF patients ($P = 0.001$ and $\eta^2 = 0.123$; Fig. 2E).

Individual or coupled spike rates were not related to clinical epilepsy parameters such as age, epilepsy duration and frequency of seizures (see Supplementary Fig. 2A–C, $P > 0.05$). Also, the coupled rates were comparable between patients with and those without MRI lesions (Supplementary Fig. 2D) as well as between patients who had resective surgery and those who had RNS (Supplementary Fig. 2E). None of the comparisons yielded a significant difference between groups (Wilcoxon, $P > 0.05$).

Previous studies emphasized the importance of sites with high spike rates to epileptogenicity and seizure outcome,[6,9,13] and in the current study, the absence of differences in aforementioned results could be masked by many sites with few or no spikes. Thus, for this reason we restricted our analysis to the 10% of contacts showing the highest spike rates per patient and compared the proportion of contacts that had high rates and high power. No significant difference was found between SF and NSF ($P = 0.117$, Fig. 2B, upper row), but there was a higher percentage of contacts in the lateral temporal region with high rates and power in NSF than SF patients ($P = 0.014$, Cliff's $d = 0.582$, Fig. 2B, lower row).

Since we included inter-contact distance in our statistical model (see 'Material and methods' section), we further quantified the effect of distance on coupled spike rates, and overall, we found longer inter-contact Euclidean distances were weakly correlated with higher normalized coupled spike rates ($|r| = 0.282$, Supplementary Fig. 3A). On an individual patient level, only three patients showed a moderate to strong correlation

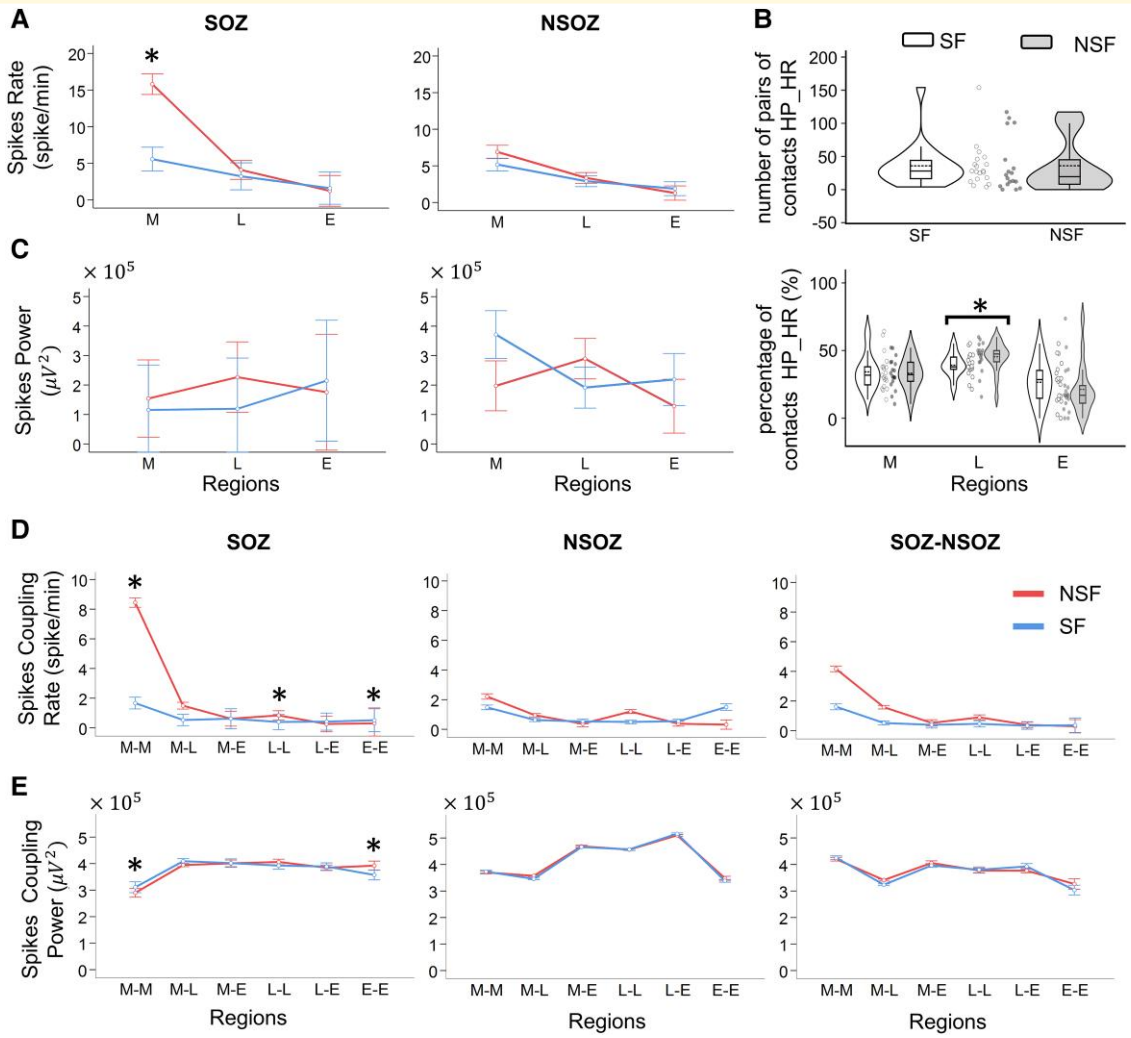

Figure 2 Spike rates in seizure onset zone (SOZ) and different brain regions. (**A**) Non-normalized spike rates for different brain regions (M: mesial temporal, L: lateral temporal and E: extra-temporal lobe) in the SOZ (left) and non-seizure onset zone (NSOZ, right) of seizure-free (SF) and not seizure-free patients (NSF). Spike rates were higher in M SOZ of NSF than SF patients (*$P < 0.001$; effect size $\eta^2 = 0.138$, MANCOVA). (**B**) Violin plots of the number of pairs of electrodes with high-coupled power and high-coupled rates (HP_HR) in SF and NSF patients (upper plot), and percentage of contacts pairs with high-coupled power and high-coupled spike rates with respect to M, L and E regions (lower plot). Note the higher percentage of contacts in L of NSF than SF patients (*$P = 0.0144$, Cliff's $d = 0.582$, Wilcoxon), each data point corresponds to one patient. (**C**) Same as **A** but spike power. In **A** and **B**, each datapoint corresponds to spike rates/power of one channel. Check Supplementary Table 4 for exact numbers of datapoints. (**D**) Non-normalized coupled spike rates for channels pairs in relation to brain region (e.g. M–M: both channels are in M, M–L: one in M and the other in L, see Supplementary material for abbreviation list) and in SOZ, NSOZ, and between SOZ and NSOZ of SF and NSF patients. In M–M (*$P < 0.001$, $\eta^2 = 0.195$, MANCOVA), L–L (*$P < 0.001$, $\eta^2 = 0.113$, MANCOVA) and E–E (*$P = 0.018$, $\eta^2 = 0.102$, MANCOVA) SOZ, coupled spike rates were higher in NSF than SF. (**E**) Same as panel **D**, but non-normalized coupled spike power. In M–M (*$P = 0.002$, $\eta^2 = 0.124$, MANCOVA) and E–E (*$P = 0.001$, $\eta^2 = 0.123$, MANCOVA), higher power in NSF than SF patients. The error bars represent 95% confidence interval. Bonferroni correction with $n = 6$ and 18 was used for individual and coupled spike rates and power comparisons, respectively. In **D** and **E**, each data point corresponds to either coupled rate or coupled power of a single channel pair. Check Supplementary Table 5 for exact numbers of datapoints.

($|r| > 0.5$), while the majority of the patients (66.6%) showed weak correlation ($|r| < 0.25$; see Supplementary Fig. 3A colour bar). Likewise, longer inter-contact distances were weakly correlated with higher normalized coupled spike power ($|r| = 0.168$, Supplementary Fig. 3B), and each of the 37 patients had a moderate to weak correlation $|r| < 0.5$ (see Supplementary Fig. 3B, colour bar).

Propagating spike sequences

Analysis of spike propagation was performed in 30 out of the 37 patients and 7 were excluded because spike propagation did not meet criteria (see 'Spikes sequences: temporal and spatial clustering' subsection in the 'Materials and methods' section). In these 30 patients, we excluded 22.6% of all

detected sequences due to volume conduction, which was defined as spikes within 2 ms of each other or 'ties'.[12] We performed multiple spike sequence analyses, adjusting the duration for when a spike could join a sequence (50 and 100 ms). Results were similar between both analyses; thus, results are only presented for a duration of 50 ms. A mean of 140.2 ± 350.1 propagating sequences were detected per patient with a range of 7–1891 sequences.

NSF patients had a significantly higher rate of spike propagation sequences (per second) than SF (Wilcoxon, $P = 0.020$; Fig. 3A) and a higher average number of spikes per sequence (Wilcoxon, $P = 0.011$; Fig. 3B) than SF patients. The average propagation time P_T between seizure outcome groups was not different (Wilcoxon, $P = 0.158$; Fig. 3C). The average total Euclidean distance associated with all spike sequences was significantly longer in NSF than SF patients (Wilcoxon, $P = 0.009$; Fig. 3D). The average distance between high-rate contacts (i.e. contacts with spike rates within the top 10% of all contacts with spikes) and leading contacts to SOZ centroid did not show a significant difference with respect to seizure outcome (Wilcoxon, $P = 0.481$ and $P = 0.089$; Fig. 3E and F, respectively).

All spikes were also clustered according to their spatial distribution. Thirteen patients had 2 spike clusters, 14 had 3 clusters and 3 had 4 clusters. The distance between the dominant cluster (i.e. cluster with highest number of spikes) and the nearest SOZ contact was comparable between the SF and NSF patients (Wilcoxon, $P = 0.354$; Fig. 3I).

We calculated the percentage of the contacts that contained high spike rates and initiated or lead a spike propagation sequence (or hiRL contacts). Results showed NSF patients had at least 37.5% hiRL contacts, but there were several SF patients who had a lower percentage. Overall, there was a significantly higher percentage of hiRL contacts in NSF than SF patients (Wilcoxon, $P = 0.0026$; Fig. 3G). These results were then analysed in relation to SOZ and seizure outcome where we found a higher percentage of hiRL contacts in the NSOZ of NSF than SF patients ($P = 0.017$), but the percentages were similar in the SOZ between outcome groups ($P = 0.342$). The hiRL and spike rates in general, in SOZ and NSOZ, were not affected by age, duration of epilepsy, presence of lesion or surgery type (see Supplementary Table 6).

Lead-downstream matrix was constructed, which quantifies how often a contact is downstream appears in a spike sequence to each contact that leads a sequence. In general, the number of leading contacts and downstream contacts were significantly higher in NSF patients reflecting the higher number of sequences. When the leading electrode and downstream were in SOZ or NSOZ, NSF patients had a significantly higher number of leading contacts than SF patients (Wilcoxon, $P = 0.041$ and 0.043, respectively; Fig. 3K). For downstream contacts, there was a significant difference between SF and NSF only when both leading and downstream electrodes are in NSOZ (Wilcoxon, $P = 0.036$; Fig. 3L).

Lastly, we used graph theory measures on directed lead-downstream matrix and found global efficiency, the inverse of the shortest path length between contacts, was significantly lower in SF than NSF patients (Wilcoxon, $P = 0.014$; Fig. 3H). The other graph theory measures of modularity, clustering coefficient and centrality were not statistically different with respect to seizure outcome.

Outcome prediction

We assessed if spike measures could predict seizure outcome using a feedforward machine learning algorithm. Single or coupled spike rates were not effective in predicting outcome. Bootstrapping of 30 patients that was repeated 1000 times resulted in confidence intervals of the AUC for single spike rates confidence interval (CI) = [0.510, 0.517] (see Fig. 4C) and for coupled spike rates CI = [0.563, 0.569] (see Fig. 4D). However, when the bootstrapping of 25 patients was used on the hiRL, the feedforward algorithm was able to separate seizure outcomes reasonably well with a CI for AUC of [0.678, 0.721] (see Fig. 4A and B).

Discussion

The current study found higher individual and coupled spike rates on electrode contacts chiefly in the mesial temporal SOZ of NSF than SF patients. There was a higher percentage of hiRL (i.e. electrodes with high spike rates and the first or leading spike of a propagated series) in the NSOZ of NSF than SF patients. The hiRL in the NSOZ of NSF patients contained a greater number of spikes that propagated over longer distances and was associated with a higher global efficiency than SF patients. Lastly, the measure of hiRL in SOZ and NSOZ, but not rate of spikes, performed well in classifying a patient's seizure outcome. These results suggest brain regions where spikes frequently propagate from could inform the extent of the seizure network that in some cases extends beyond the SOZ, and the extent of hiRL contains information that predicts whether a surgical patient will be seizure free.

Sources of inter-ictal and ictal discharges

The spatial relationship between spikes and SOZ has been extensively studied in patients with temporal and extra-temporal epilepsy.[3,12,23-27] Results from these studies and others suggest information about spikes, such as rate or extent of spike propagation, are associated with the SOZ[3,10,25,28] or epileptogenic zone.[6,13,29] Some studies found spikes strongly localize the SOZ,[3,30] and others show the rate or extent of propagation can predict seizure freedom.[14,31] In the current study of chiefly temporal lobe epilepsy, we, too, found higher individual spike rates in mesial temporal SOZ and coupled rates in, but not between, brain regions of SOZ of NSF patients than SF patients. The latter result could be evidence of segregation in the seizure network, which others have found in resting state functional

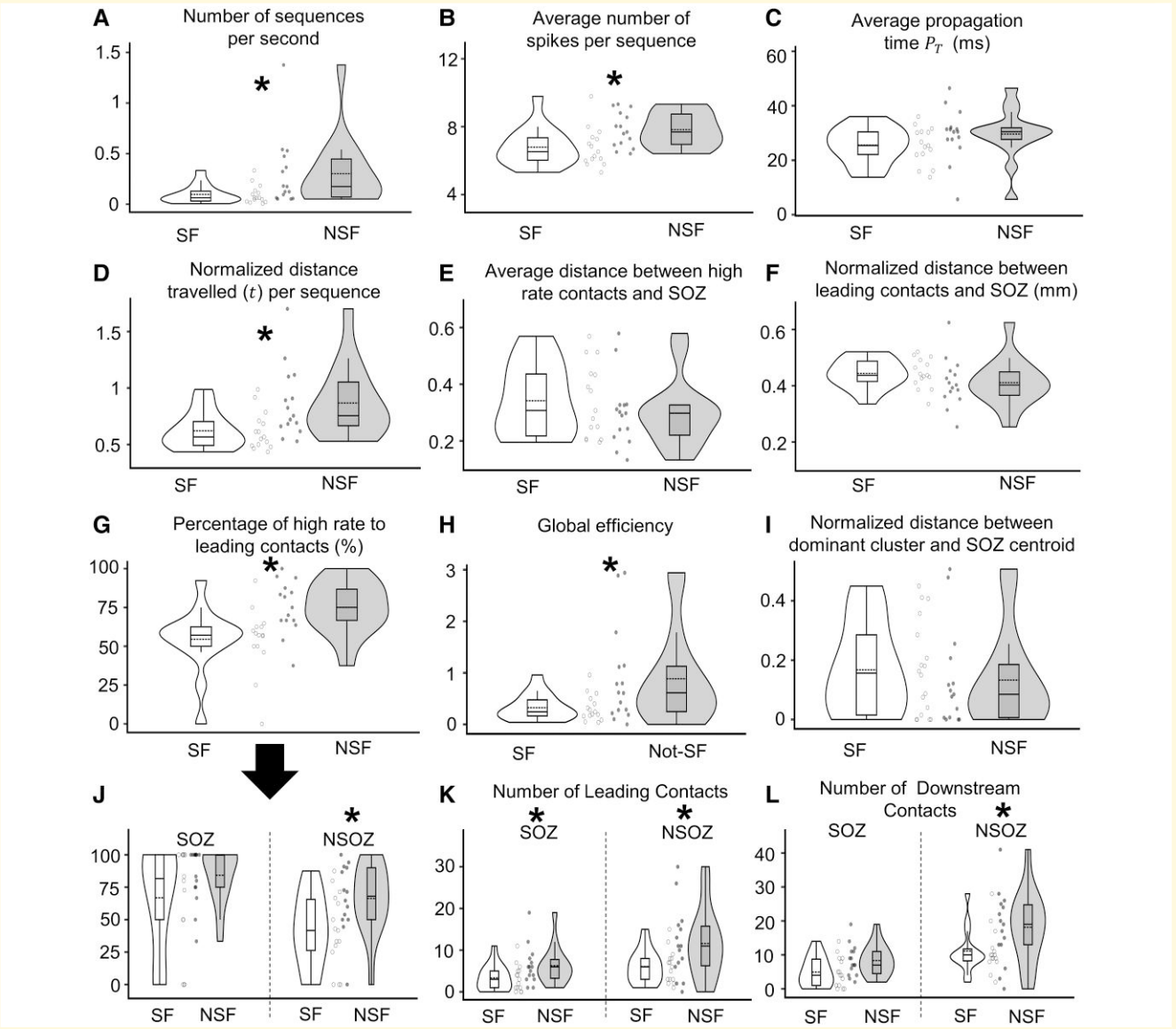

Figure 3 Comparison of spike propagation measures between seizure-free (SF) and not seizure-free (NSF) patients. Violin plots of the number of spike sequences per second (**A**; Wilcoxon, $P = 0.020$, Cliff's $d = 0.502$), average number of spikes per sequence (**B**; Wilcoxon, $P = 0.011$, $d = 0.547$), average propagation time P_T, which is the time between the occurrence of the leader spike and the last spike in the sequence (**C**), normalized Euclidean distance (t) (**D**; Wilcoxon, $P = 0.009$, $d = 0.145$), average normalized distance between channels with the highest 10% rates and the centroids of the seizure onset zone (SOZ) (**E**), same as panel **E** but for the leading channels (**F**), percentage of the leading contacts that also have high spike rates (**G**; Wilcoxon, $P = 0.003$, $d = 0.649$), global efficiency (inverse of shortest path length) derived from the leading-downstream matrix (**H**; Wilcoxon, $P = 0.014$, $d = 0.392$), normalized distance between dominant spike cluster (cluster that has the highest number of sequences) and the centroid of the SOZ (**I**), same as panel **G**, but values for SOZ and non-seizure onset zone or NSOZ (**J**; Wilcoxon, $P = 0.017$, $d = 0.673$ for NSOZ), number of leading channels with respect to the SOZ and NSOZ (**K**; Wilcoxon, $P = 0.041$, 0.043 and $d = 0.781$, 0.356 for SOZ and NSOZ, respectively), and number of downstream channels in SOZ and NSOZ (**L**; Wilcoxon, $P = 0.036$ and $d = 0.435$ for NSOZ). In all plots, each datapoint corresponds to a measure from one patient. Asterisks (∗) represent significant differences between SF and NSF groups. $n = 30$ was used in all comparisons.

connectivity studies and could be an adaptation of the interictal state opposing the transition to ictus.[32] While higher rates could indicate NSF patients had a severe form of epilepsy[33] that was irremediable by resection or stimulation, rates alone provided little prognostic value since the rate of individual or coupled spikes performed near chance in classifying seizure outcome. In contrast to rates, there were a significantly higher proportion of hiRL in NSF than SF patients. Recent work suggests spikes are travelling waves that emerge from a local source, which can be the same location where ictal discharges emerge from or travel to or both.[10,14] Based on these previous studies and in the current work, if

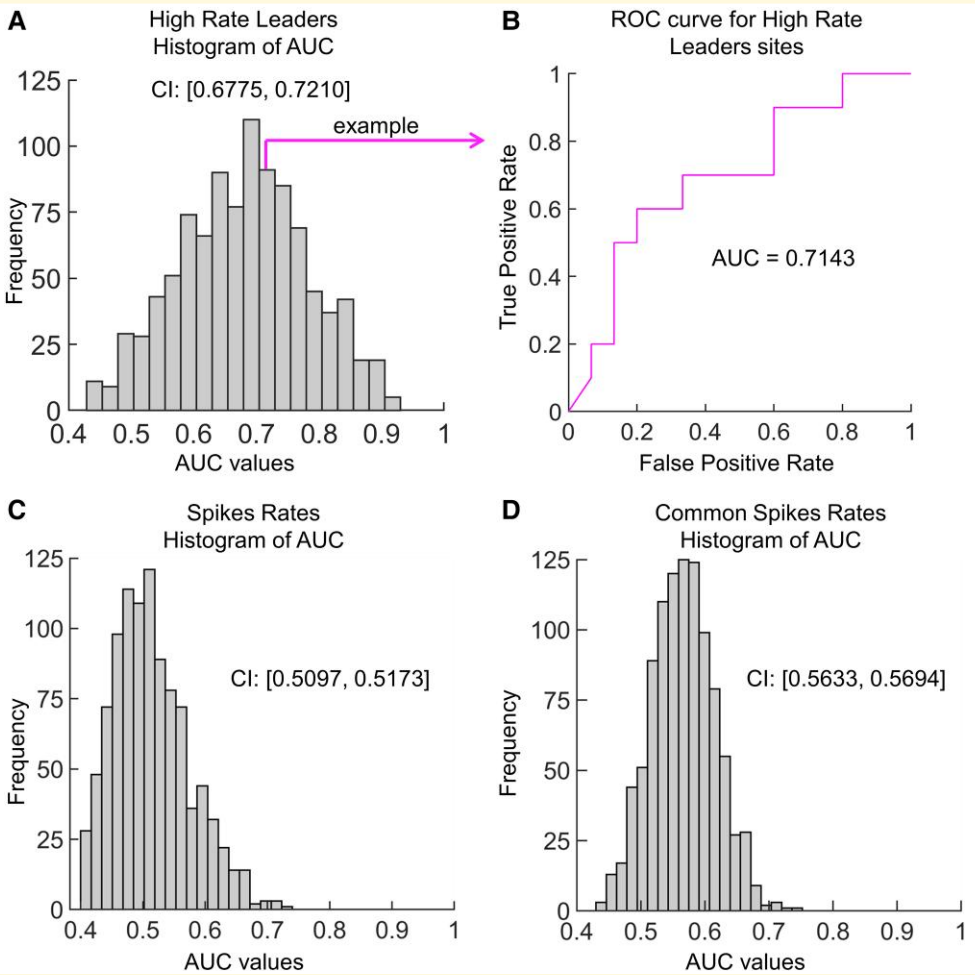

Figure 4 Receiver operating characteristic (ROC) curves to predict seizure outcome. (**A**) Histogram of area under curve (AUC) values for 1000 iterations of the feedforward model using high-rate leaders (hiRL) to predict seizure outcome. Each iteration used a leave-one-out method where 24 randomly selected patients were used to train and 1 patient was used to test the model. (**B**) ROC curve illustrating one iteration, which had an AUC value of 0.7143. (**C** and **D**) Same as panel **A** but using individual (**C**) and coupled spike rates (**D**). In these analyses, the leave-one-out method used 29 randomly selected patients to train and 1 patient to test the model. The confidence interval (CI) is shown besides each histogram.

the electrodes with hiRL are at or nearest the source from which spikes emerge, then hiRL could be associated with sources that generate and/or propagate ictal discharges. We did find hiRL were associated with the clinical SOZ of all patients, but more were found in the NSOZ of NSF than SF patients. These results indicate in many of the NSF patients, some hiRL could be near sources that generate ictal discharges, which were unidentified during the invasive EEG test, and the tissue surrounding electrodes with hiRL needs to be remove, disconnected or stimulated to control seizures.[14] Consistent with this hypothesis was the result that the extent of hiRL in the SOZ and NSOZ was informative and could accurately classify seizure outcome (AUC = 0.699). This performance is comparable in accuracy to other methods predicting seizure outcome based on spike-related measures like cross rates of spikes and high-frequency oscillations (80–500 Hz),[34] rate of spikes with preceding gamma activity,[35] spatiotemporal dynamics of spikes[36] and spike networks.[13] Also, supporting the aforementioned hypothesis are a series of EEG-fMRI studies of temporal and extra-temporal epilepsy that show regions with the maximum haemodynamic response are often the source where spikes originate,[26] the maximum haemodynamic response often localizes the SOZ[37] and complete removal of regions with the maximal haemodynamic response was found in SF patients, and resected volumes lacking the maximum response were more often found in NSF patients.[38] Collectively, the current and previous studies highlight the translational implications of detecting sources of spikes that could help inform the seizure network.

Study design considerations

Readers of the current results should consider the patient sample size ($n = 18$ SF and $n = 19$ NSF) and differences between groups with respect to duration of epilepsy, which was longer in SF than NSF patients. If we assume a longer duration of epilepsy contributes to higher spike rates, then

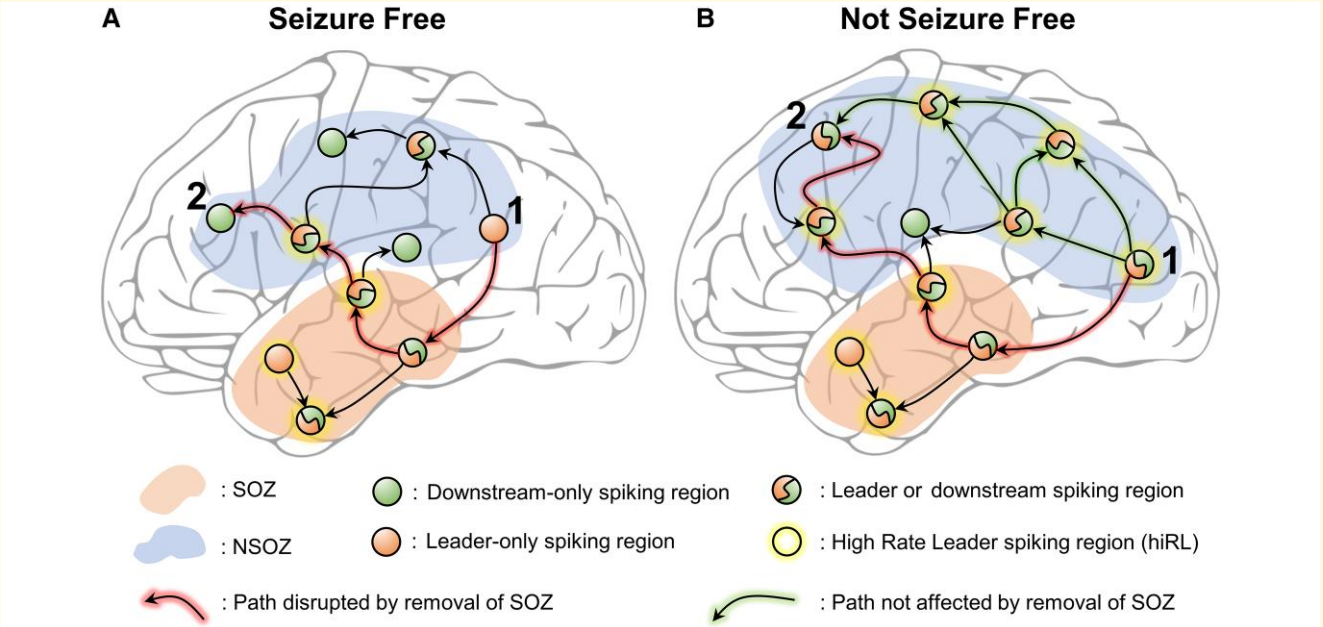

Figure 5 A high-rate leader (hiRL)-dominated spike network that could support seizures. (**A**) A schematic illustrating a hypothesized spike network in seizure-free patients. In the seizure onset zone (SOZ, area shaded light red), there are many hiRL (circles with yellow halo) and in non-SOZ (NSOZ, area shaded blue), a single hiRL is represented. Regions that lead or are downstream in spike sequences are denoted by orange- and green-filled circles. The number of regions that generate or propagate spikes and the number of hiRL affects the efficiency of the network. The path between regions 1 and 2 (arrows highlighted in red) is disrupted if the SOZ is removed or treated. (**B**) Same as **A** but for not seizure-free patients. There are many hiRL that can lead or are downstream in spike sequences. Unlike the single path between regions 1 and 2 in seizure-free patient in panel **A**, there are multiple paths for spike propagation between regions 1 and 2 in not seizure-free patients, and removal of the SOZ only disrupts one path, while alternative paths remain for spike propagation (arrows highlighted in green).

SF patients should have higher rates than NSF; yet, the opposite was found in the current study. Moreover, there was no correlation between duration of epilepsy and rates in relation to SOZ. In 11 patients, we could confirm resection of the SOZ using post-surgical MRI (see Supplementary Fig. 4) and in the remaining patients, we had to rely upon collected tissue specimens documented in the pathology report and the neurosurgeon's notes as evidence the SOZ was removed, which might not be as accurate as MRI. Although the majority of patients had resective surgery, there were eight patients (three seizure free, five not seizure free) who received VNS or RNS treatment, which could affect the time course of seizure control and thus seizure outcome. If we consider seizure outcome to correspond with how much of SOZ was resected or treated, then there was no difference in outcomes between patients who had surgery versus those who had VNS or RNS (Fisher's exact test, two-tailed, $P = 0.430$). Another important consideration is analysis used 10-min inter-ictal recordings early in the patient's evaluation, which was intended to reduce factors that could affect the rate and spatial distribution of spike and potentially mask results (see 'Materials and methods' section).[12,39] Also, hiRL were not found in all patients with temporal lobe epilepsy (7 out of 37), especially those who had low spike rates and <5 spike propagation sequences. This proportion of patients is similar to a previous study of temporal and extra-temporal epilepsy that used longer recordings,[12] though future work on hiRL should assess longer duration recordings to determine whether these methods could be applied to more, if not all, patients with temporal lobe epilepsy. Lastly, our study and others like it are limited by the electrode coverage that could miss portions of the seizure network or contribute to some electrodes mislabelled as spike leaders that were actually downstream from an unsampled source.

Do spikes play a role in seizure recurrence?

Studies show inter-ictal and ictal discharges are differentially affected by state of vigilance and anti-seizure medication,[39-42] suggesting these are distinct epileptiform phenomena generated by different mechanisms.[1] Furthermore, it appears spikes have little influence on seizure occurrence,[41,43-45] and several, but not all,[46] studies indicate higher rates correlate with poor seizure outcome in temporal lobe epilepsy.[6,33,47] Based on these data and current results it is reasonable to ask what role, if any, could hiRL play in seizure recurrence after surgery? This study nor others like it provide no direct evidence; however, recent work shows there are variable sources generating spikes and ictal discharges,[10,48] and as previously noted sources of spikes are often the same location where ictal discharges emerge from or propagate to, which could be due

to a combination of hyper-excitability and lower seizure threshold that facilitates spike sources to be recruited during a seizure.[14] Despite evidence for segregation in the SOZ, our results show regions with hiRL generate spikes that could be a leader during one propagated sequence and downstream during another sequence, and there were more hiRL with this dual functionality in the NSOZ of NSF than SF patients (Fig. 5A and B). This feature of hiRL could an effective mechanism that actively propagate spikes and could explain the higher global efficiency of propagation in NSF than SF patients (Fig. 2H). If we assume the seizure network contains brain regions where seizure begin and spread, and the hiRL co-localize with the seizure network, then in many surgical patients with few hiRL, removing or disconnecting all or most of the SOZ eliminates seizures. However, in some patients with many hiRL, the same therapy does not control seizures because there is an extensive and efficient hiRL-dominated network beyond the SOZ that can support the generation and spread of seizures.

Conclusion and future work

Accurate localization of the brain regions responsible for generating seizures and prediction of response to therapy are important to improve treatment of epilepsy. The current work shows the extent of hiRL could inform the location of the seizure network, which can include more than the clinical SOZ, and can predict seizure outcome after resective surgery or stimulation. We believe there are different types of spikes with different functionality in and outside the seizure network, and future work characterizing spikes and slow wave features, investigating the neuronal basis of spikes, and correlation between spikes other electrophysiological disturbances such as pathological high-frequency oscillations could help to classify spikes and their function(s) with respect to the seizure network.

Supplementary material

Supplementary material is available at *Brain Communications* online.

Funding

This study was supported by the National Institutes of Health (NIH) grant NS106957 (R.J.S.), 033310 (J.E.) and Christina Louise George Trust.

Competing interests

The authors report no competing interests.

Data availability

The data that support the findings of this study are available from the corresponding author, upon reasonable request.

References

1. Gotman J. Relationships between interictal spiking and seizures: Human and experimental evidence. *Can J Neurol Sci*. 1991; 18(Suppl 4):573-576.
2. Alarcon G, Guy CN, Binnie CD, Walker SR, Elwes RD, Polkey CE. Intracerebral propagation of interictal activity in partial epilepsy: Implications for source localisation. *J Neurol Neurosurg Psychiatry*. 1994;57(4):435-449.
3. Marsh ED, Peltzer B, Brown MW, *et al*. Interictal EEG spikes identify the region of electrographic seizure onset in some, but not all, pediatric epilepsy patients. *Epilepsia*. 2010;51(4):592-601.
4. Alarcon G, Garcia Seoane JJ, Binnie CD, *et al*. Origin and propagation of interictal discharges in the acute electrocorticogram. Implications for pathophysiology and surgical treatment of temporal lobe epilepsy. *Brain*. 1997;120(Pt 12):2259-2282.
5. Schulz R, Lüders HO, Hoppe M, Tuxhorn I, May T, Ebner A. Interictal EEG and ictal scalp EEG propagation are highly predictive of surgical outcome in mesial temporal lobe epilepsy. *Epilepsia*. 2000;41(5):564-570.
6. Krendl R, Lurger S, Baumgartner C. Absolute spike frequency predicts surgical outcome in TLE with unilateral hippocampal atrophy. *Neurology*. 2008;71(6):413-418.
7. Villanueva V, Peral E, Albisua J, de Felipe J, Serratosa JM. Prognostic factors in temporal lobe epilepsy surgery. *Neurologia*. 2004;19(3):92-98.
8. Hufnagel A, Elger CE, Pels H, *et al*. Prognostic significance of ictal and interictal epileptiform activity in temporal lobe epilepsy. *Epilepsia*. 1994;35(6):1146-1153.
9. Janszky J, Schulz R, Hoppe M, Ebner A. Spikes on the postoperative EEG are related to preoperative spike frequency and postoperative seizures. *Epilepsy Res*. 2003;57(2–3):153-158.
10. Smith EH, Liou JY, Merricks EM, *et al*. Human interictal epileptiform discharges are bidirectional traveling waves echoing ictal discharges. *eLife*. 2022;11:e73541.
11. Maharathi B, Patton J, Serafini A, Slavin K, Loeb JA. Highly consistent temporal lobe interictal spike networks revealed from foramen ovale electrodes. *Clin Neurophysiol*. 2021;132(9):2065-2074.
12. Conrad EC, Tomlinson SB, Wong JN, *et al*. Spatial distribution of interictal spikes fluctuates over time and localizes seizure onset. *Brain*. 2020;143(2):554-569.
13. Azeem A, von Ellenrieder N, Hall J, Dubeau F, Frauscher B, Gotman J. Interictal spike networks predict surgical outcome in patients with drug-resistant focal epilepsy. *Ann Clin Transl Neurol*. 2021;8(6): 1212-1223.
14. Diamond JM, Withers CP, Chapeton JI, Rahman S, Inati SK, Zaghloul KA. Interictal discharges in the human brain are traveling waves arising from an epileptogenic source. *Brain*. 2023;146(5): 1903-1915. Published online February 2
15. Shamas M, Yeh HJ, Fried I, Engel J, Staba R. Interictal gamma event connectivity differentiates the seizure network and outcome in patients after temporal lobe epilepsy surgery. *eNeuro*. 2022;9(6): ENEURO.0141-22.2022.
16. Roehri N, Pizzo F, Bartolomei F, Wendling F, Bénar CG. What are the assets and weaknesses of HFO detectors? A benchmark framework based on realistic simulations. *PLoS One*. 2017;12(4):e0174702.
17. Roehri N, Lina JM, Mosher JC, Bartolomei F, Benar CG. Time-frequency strategies for increasing high-frequency oscillation detectability in intracerebral EEG. *IEEE Trans Biomed Eng*. 2016; 63(12):2595-2606.
18. Blenkmann AO, Phillips HN, Princich JP, *et al*. Ielectrodes: A comprehensive open-source toolbox for depth and subdural grid electrode localization. *Front Neuroinform*. 2017;11:14.
19. González-Burgos G, Barrionuevo G, Lewis DA. Horizontal synaptic connections in monkey prefrontal cortex: An in vitro electrophysiological study. *Cereb Cortex*. 2000;10(1):82-92.
20. Cohen J. *Statistical power analysis for the behavioral sciences*. 2nd edn. Routledge; 1988.

21. *IBM SPSS statistics for windows*. IBM Corp; 2020.
22. Auer P, Burgsteiner H, Maass W. A learning rule for very simple universal approximators consisting of a single layer of perceptrons. *Neural Netw*. 2008;21(5):786-795.
23. Dahal P, Ghani N, Flinker A, *et al*. Interictal epileptiform discharges shape large-scale intercortical communication. *Brain*. 2019; 142(11):3502-3513.
24. Ung H, Cazares C, Nanivadekar A, *et al*. Interictal epileptiform activity outside the seizure onset zone impacts cognition. *Brain*. 2017; 140(8):2157-2168.
25. Numata-Uematsu Y, Uematsu M, Sakuraba R, *et al*. The onset of interictal spike-related ripples facilitates detection of the epileptogenic zone. *Front Neurol*. 2021;12:724417.
26. Khoo HM, von Ellenrieder N, Zazubovits N, He D, Dubeau F, Gotman J. The spike onset zone: The region where epileptic spikes start and from where they propagate. *Neurology*. 2018;91(7): e666-e674.
27. Bartolomei F, Trébuchon A, Bonini F, *et al*. What is the concordance between the seizure onset zone and the irritative zone? A SEEG quantified study. *Clin Neurophysiol*. 2016;127(2): 1157-1162.
28. Gaspard N, Alkawadri R, Farooque P, Goncharova II, Zaveri HP. Automatic detection of prominent interictal spikes in intracranial EEG: Validation of an algorithm and relationship to the seizure onset zone. *Clin Neurophysiol*. 2014;125(6): 1095-1103.
29. King-Stephens D. Do interictal rates influence treatment outcomes in temporal lobe epilepsy? *Epilepsy Curr*. 2020;20(2):83-84.
30. Asano E, Muzik O, Shah A, *et al*. Quantitative interictal subdural EEG analyses in children with neocortical epilepsy. *Epilepsia*. 2003;44(3):425-434.
31. Bear JJ, Kirsch HE, Berman BD, Chapman KE, Tregellas JR. Spike-associated networks and intracranial electrographic findings. *Epileptic Disord*. 2020;22(3):291-299.
32. Pedersen M, Omidvarnia AH, Walz JM, Jackson GD. Increased segregation of brain networks in focal epilepsy: An fMRI graph theory finding. *Neuroimage Clin*. 2015;8:536-542.
33. Rosati A, Aghakhani Y, Bernasconi A, *et al*. Intractable temporal lobe epilepsy with rare spikes is less severe than with frequent spikes. *Neurology*. 2003;60(8):1290-1295.
34. Roehri N, Pizzo F, Lagarde S, *et al*. High-frequency oscillations are not better biomarkers of epileptogenic tissues than spikes. *Ann Neurol*. 2018;83(1):84-97.
35. Thomas J, Kahane P, Abdallah C, *et al*. A subpopulation of spikes predicts successful epilepsy surgery outcome. *Ann Neurol*. 2023; 93(3):522-535.
36. Klimes P, Peter-Derex L, Hall J, Dubeau F, Frauscher B. Spatio-temporal spike dynamics predict surgical outcome in adult focal epilepsy. *Clin Neurophysiol*. 2022;134:88-99.
37. Khoo HM, Hao Y, von Ellenrieder N, *et al*. The hemodynamic response to interictal epileptic discharges localizes the seizure-onset zone. *Epilepsia*. 2017;58(5):811-823.
38. An D, Fahoum F, Hall J, Olivier A, Gotman J, Dubeau F. Electroencephalography/functional magnetic resonance imaging responses help predict surgical outcome in focal epilepsy. *Epilepsia*. 2013;54(12):2184-2194.
39. Goncharova II, Alkawadri R, Gaspard N, *et al*. The relationship between seizures, interictal spikes and antiepileptic drugs. *Clin Neurophysiol*. 2016;127(9):3180-3186.
40. Matsumoto H, Marsan CA. Cortical cellular phenomena in experimental epilepsy: Interictal manifestations. *Exp Neurol*. 1964;9(4):286-304.
41. Gotman J, Marciani MG. Electroencephalographic spiking activity, drug levels, and seizure occurrence in epileptic patients. *Ann Neurol*. 1985;17(6):597-603.
42. Ng M, Pavlova M. Why are seizures rare in rapid eye movement sleep? Review of the frequency of seizures in different sleep stages. *Epilepsy Res Treat*. 2013;2013:932790.
43. Zijlmans M, Jacobs J, Zelmann R, Dubeau F, Gotman J. High frequency oscillations and seizure frequency in patients with focal epilepsy. *Epilepsy Res*. 2009;85(2–3):287-292.
44. Gotman J, Koffler DJ. Interictal spiking increases after seizures but does not after decrease in medication. *Electroencephalogr Clin Neurophysiol*. 1989;72(1):7-15.
45. Spencer SS, Goncharova II, Duckrow RB, Novotny EJ, Zaveri HP. Interictal spikes on intracranial recording: Behavior, physiology, and implications. *Epilepsia*. 2008;49(11):1881-1892.
46. Ngo L, Sperling MR, Skidmore C, Mintzer S, Nei M. Absolute spike frequency as a predictor of surgical outcome in temporal lobe epilepsy. *Seizure*. 2017;47:83-86.
47. Arcot Desai S, Tcheng TK, Morrell MJ. Quantitative electrocorticographic biomarkers of clinical outcomes in mesial temporal lobe epileptic patients treated with the RNS® system. *Clin Neurophysiol*. 2019;130(8):1364-1374.
48. Schlafly ED, Marshall FA, Merricks EM, *et al*. Multiple sources of fast traveling waves during human seizures: Resolving a controversy. *J Neurosci*. 2022;42(36):6966-6982.